Supplement of The Cryosphere, 19, 955–973, 2025
https://doi.org/10.5194/tc-19-955-2025-supplement

The Cryosphere Open Access EGU

Supplement of

Assessing the sensitivity of the Vanderford Glacier, East Antarctica, to basal melt and calving

Lawrence A. Bird et al.

Correspondence to: Lawrence A. Bird (lawrence.bird@monash.edu)

Supplementary Information

Supplementary information comprises Figures S1-S8.

Figure S1 shows changes in key model fields during the 500-year model spin-up. Figure S2 shows localised temporary ungrounding along the central flowline during the Weertman $M_{Davison}$ experiment. Figures S3 and S4 show changes in ice thickness from the M_{Paolo}, $M_{Davison}$, and C_{obs} experiments at the end of the perturbation period (Fig. S3) and the end of the simulation (Fig. S4). Figure S5 shows changes in grounded and floating ice thickness and ice velocity due to basal melt and calving perturbations. We calculate changes to grounded ice across regions that are always grounded (i.e., using the most retreated grounding line position from each simulation) and changes to floating ice across regions that are always floating (i.e. the most advanced grounding line position from each simulation). This prevents grounding line migration and calving biasing our results as the extent of ice cover and the grounding line migrates across regions of varying ice thickness. Figures S6 and S7 show changes in ice thickness and ice velocity, respectively, for M_{10}, M_{50}, and M_{100} experiments. We present these three experiments as a subset of all basal melt perturbations to demonstrate the range of simulated changes across the perturbation experiments. Figure S8 shows select results from experiments with constant melt rates (Mc; 10, 20, 30, and 40 m yr^{-1}) across all floating ice regions.

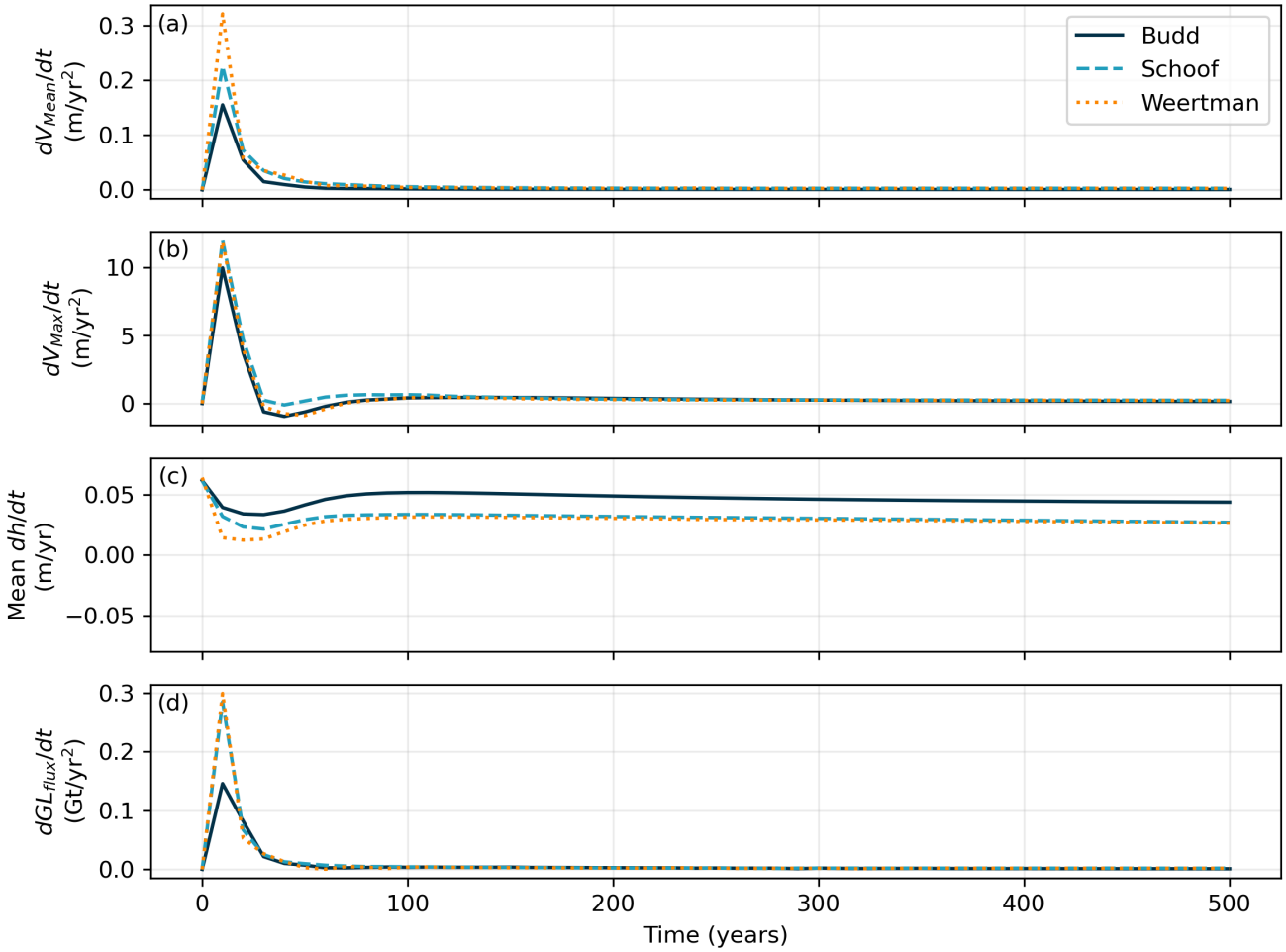

S 1: Evolution of key model fields during 500-year model spin-up. (a) Change in mean velocity over time, (b) Change in maximum velocity over time, (c) Mean change in thickness over time, (d) Change in grounding line flux over time.

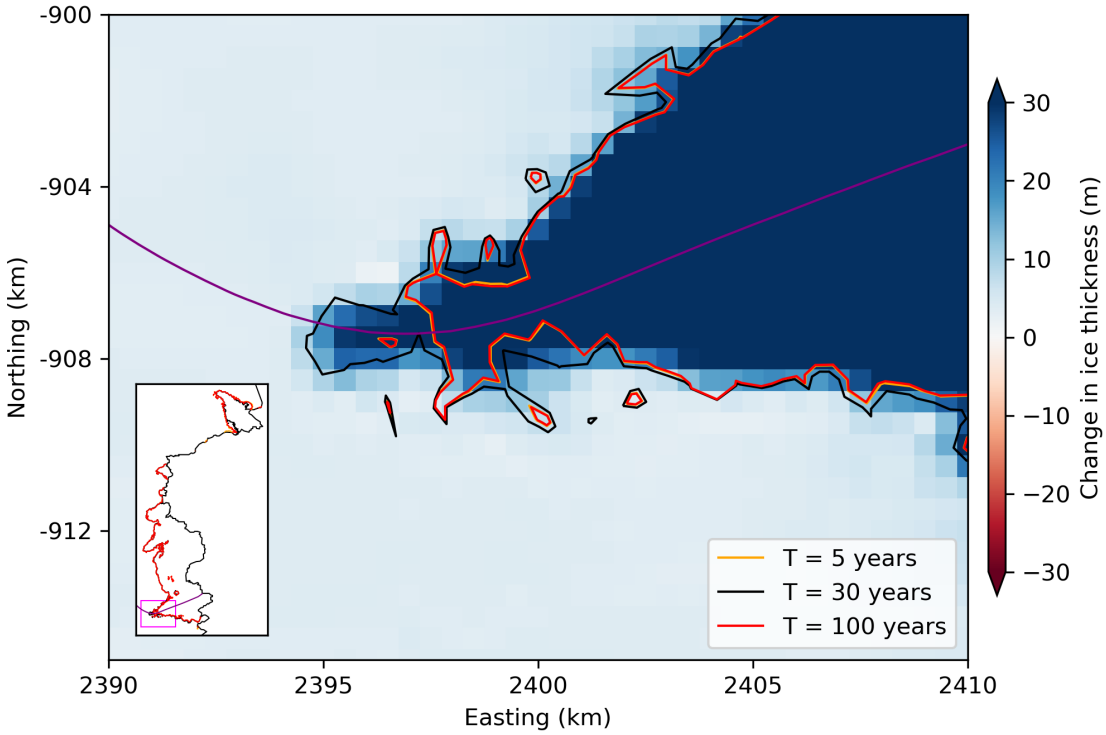

S 2: Weertman $M_{Davison}$ grounding lines and ice thickness change. Thickness change is shown as the difference between ice thickness at the end of the simulation period (T = 100 years) and at the end of the perturbation period (T = 30 years) when the grounding line is at its most retreated. Purple line denotes the flowline along which grounding retreat is calculted.

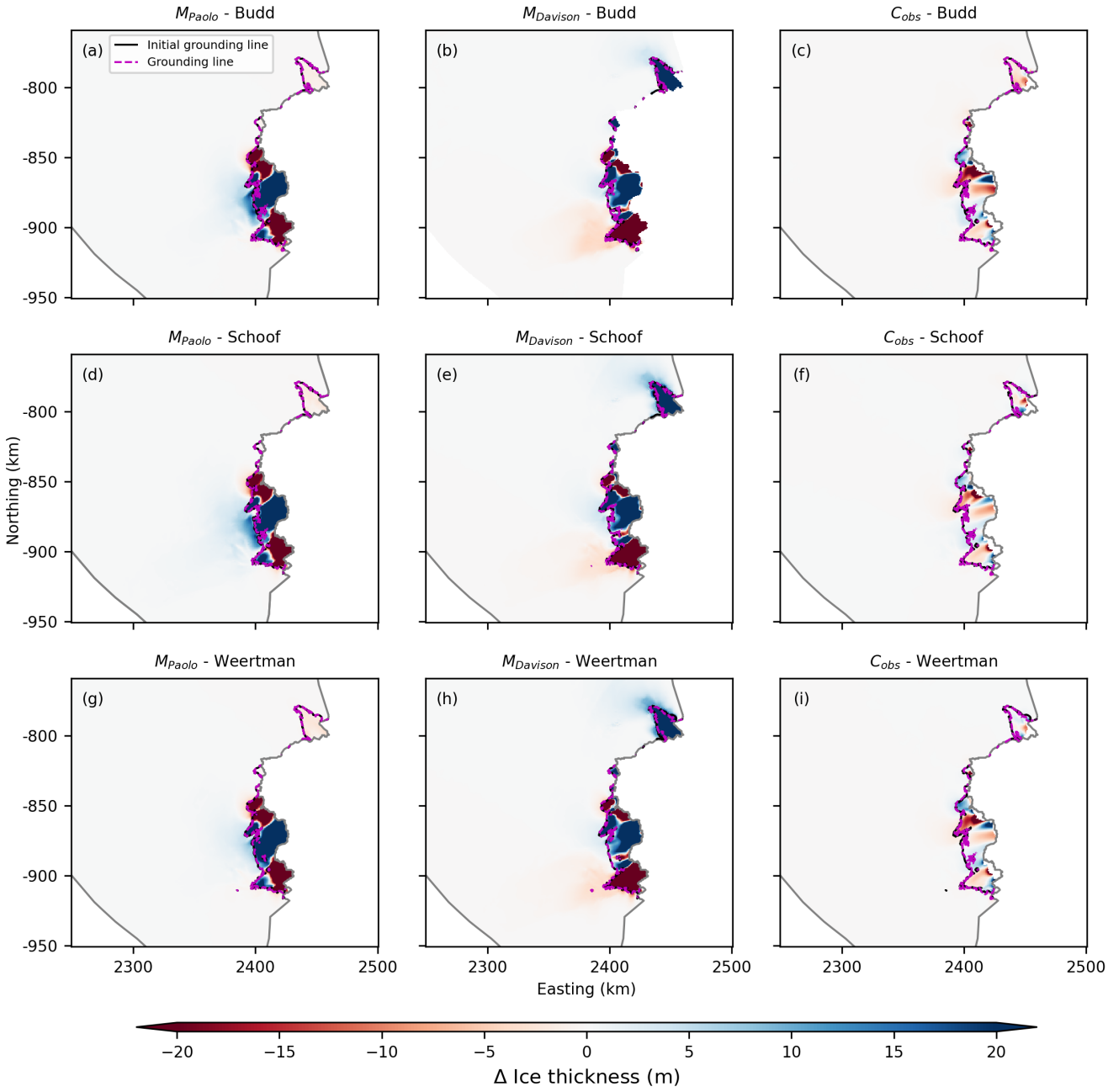

S 3: Relative change in ice thickness (compared to the *Ctrl* experiment for each friction law) at the end of the perturbation period for (a) M_{Paolo} using the Budd friction law; (b) $M_{Davison}$ for the Budd friction law; (c) C_{obs} for the Budd friction law; (d) M_{Paolo} for the Schoof friction law; (e) $M_{Davison}$ for the Schoof friction law; (f) C_{obs} for the Schoof friction law; (g) M_{Paolo} for the Weertman friction law; (h) $M_{Davison}$ for the Weertman Friction Law; and (i) C_{obs} for the Weertman friction law. The black line is the initial grounding line location at the beginning of the simulation, the magenta line is the grounding line position at the end of the perturbation period, and the grey line shows the model domain.

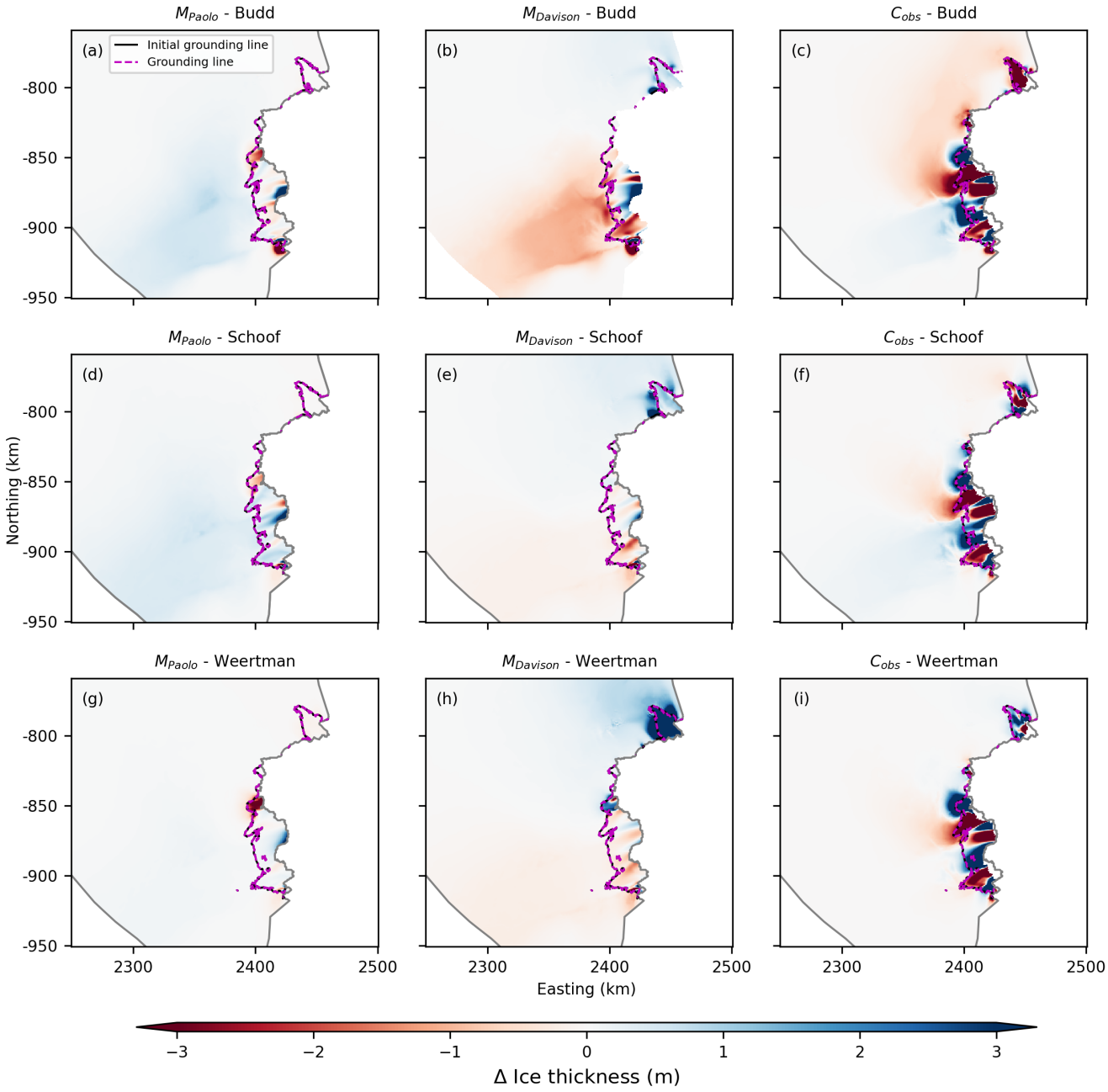

S 4: Relative change in ice thickness (compared to the *Ctrl* experiment for each friction law) at the end of the simulation for (a) M_{Paolo} using the Budd friction law; (b) $M_{Davison}$ for the Budd friction law; (c) C_{obs} for the Budd friction law; (d) M_{Paolo} for the Schoof friction law; (e) $M_{Davison}$ for the Schoof friction law; (f) C_{obs} for the Schoof friction law; (g) M_{Paolo} for the Weertman friction law; (h) $M_{Davison}$ for the Weertman Friction Law; and (i) C_{obs} for the Weertman friction law. The black line is the initial grounding line location at the beginning of the simulation, the magenta line is the grounding line position at the end of the simulation, and the grey line shows the model domain.

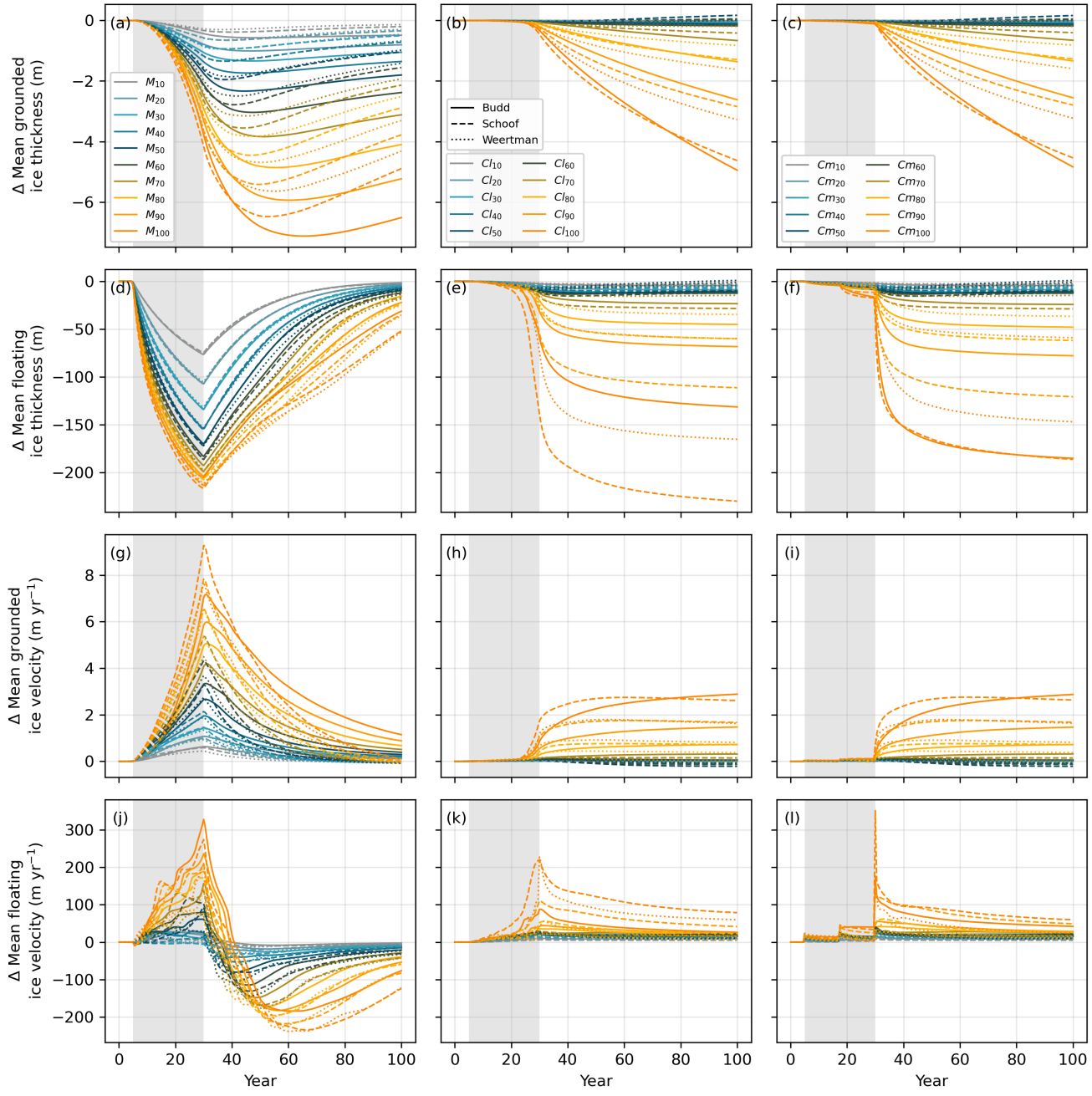

S 5: Relative change (compared to the *Ctrl* experiment for each friction law) of mean grounded ice thickness (a-c), mean floating ice thickness (d-f), mean grounded ice velocity (g-i), and floating ice velocity (j-l). Grey shaded area denotes the perturbation period.

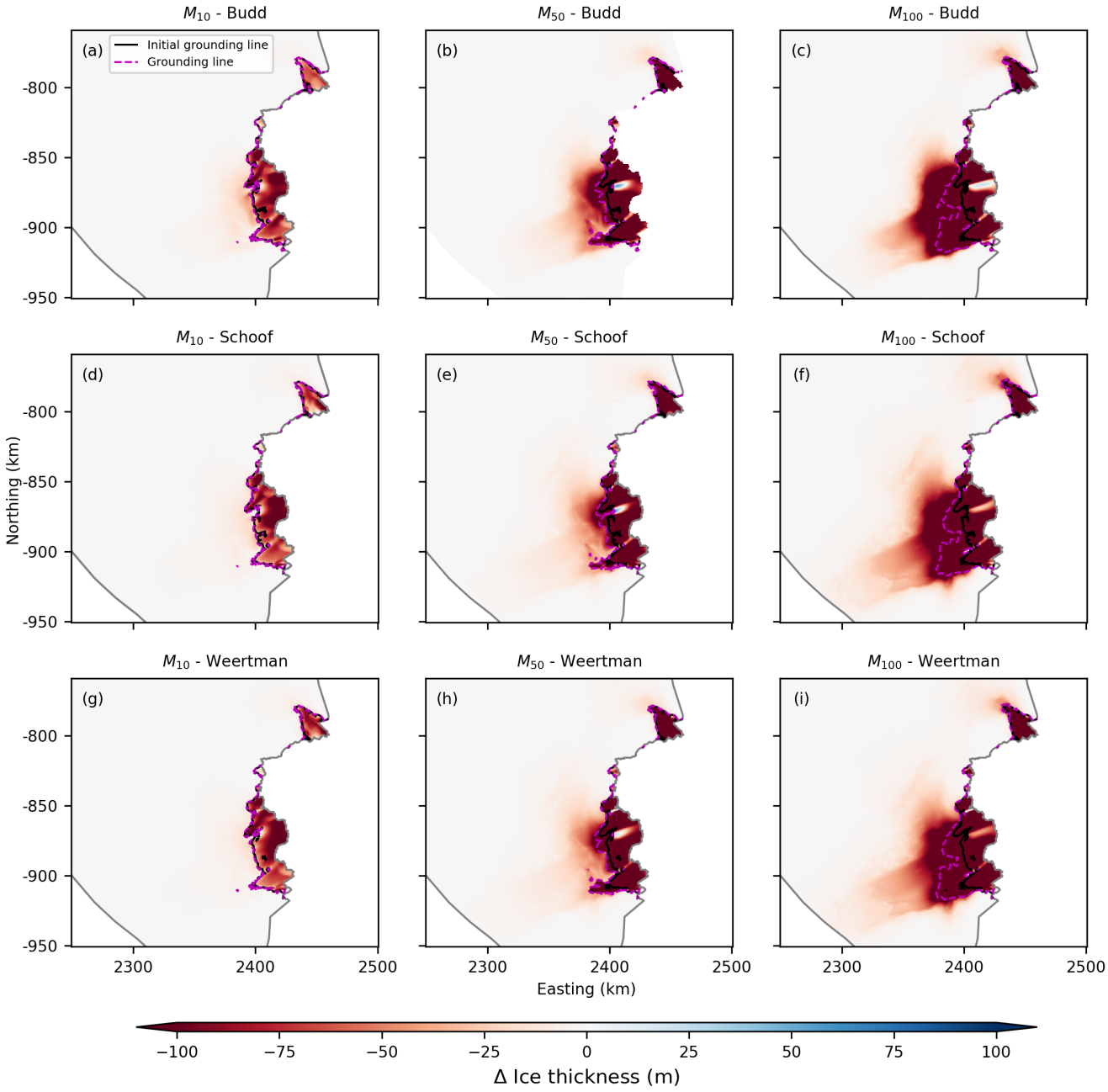

S 6: Relative change in ice thickness (compared to the *Ctrl* experiment for each friction law) at the end of the perturbation period for M_{10} (a, d, g), M_{50} (b, e, h), and M_{100} (c, f, i) experiments. Experiments using the Budd, Schoof, and Weertman friction law are shown in (a-c), (d-f), and (g-i), respectively. The black line is the initial grounding line location at the beginning of the simulation, the magenta line is the grounding line position at the end of the simulation, and the grey line shows the model domain.

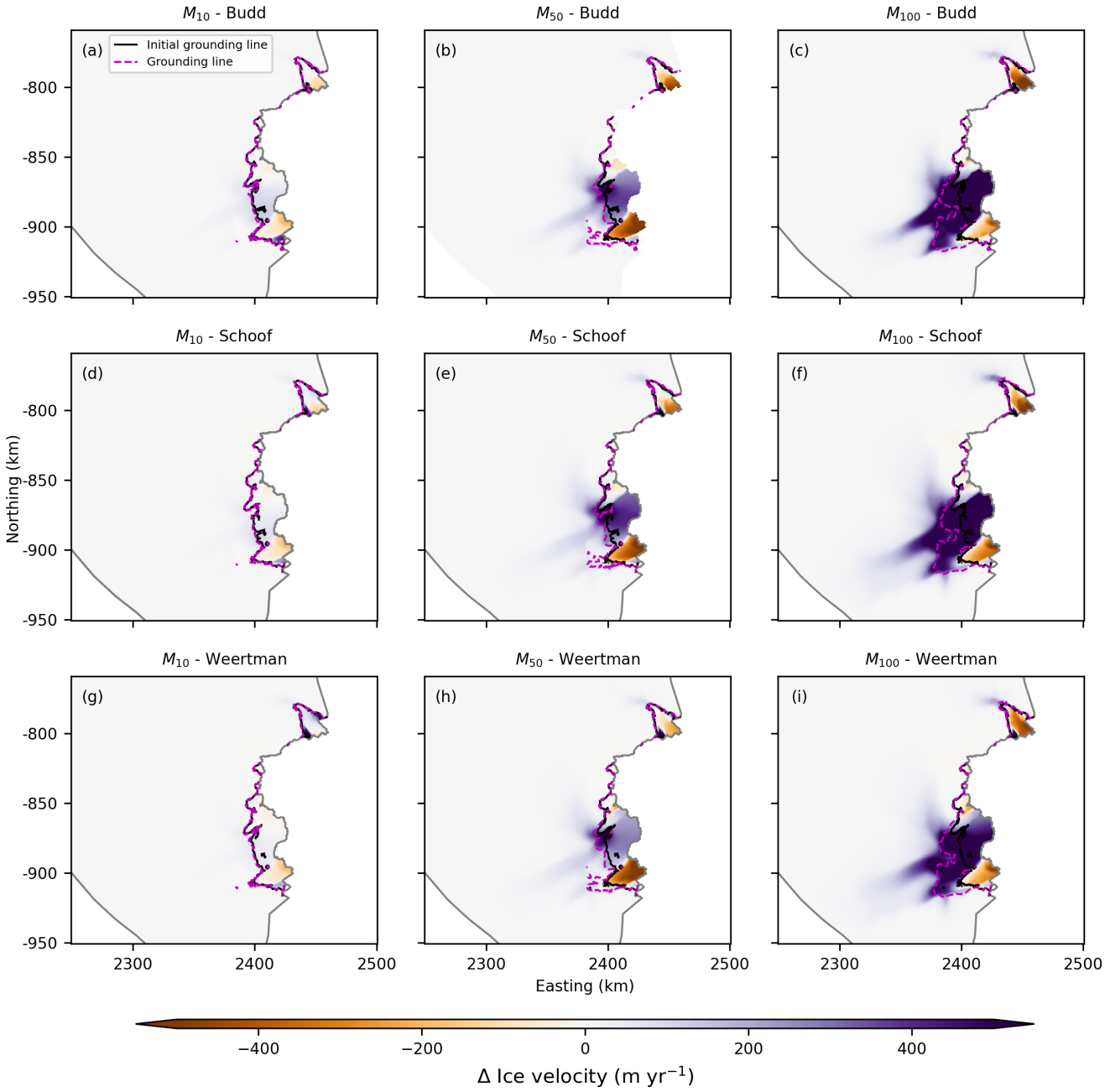

S 7: Relative change in ice velocity (compared to the *Ctrl* experiment for each friction law) at the end of the perturbation period for M_{10} (a, d, g), M_{50} (b, e, h), and M_{100} (c, f, i) experiments. Experiments using the Budd, Schoof, and Weertman friction law are shown in (a-c), (d-f), and (g-i), respectively. The black line is the initial grounding line location at the beginning of the simulation, the magenta line is the grounding line position at the end of the simulation, and the grey line shows the model domain.

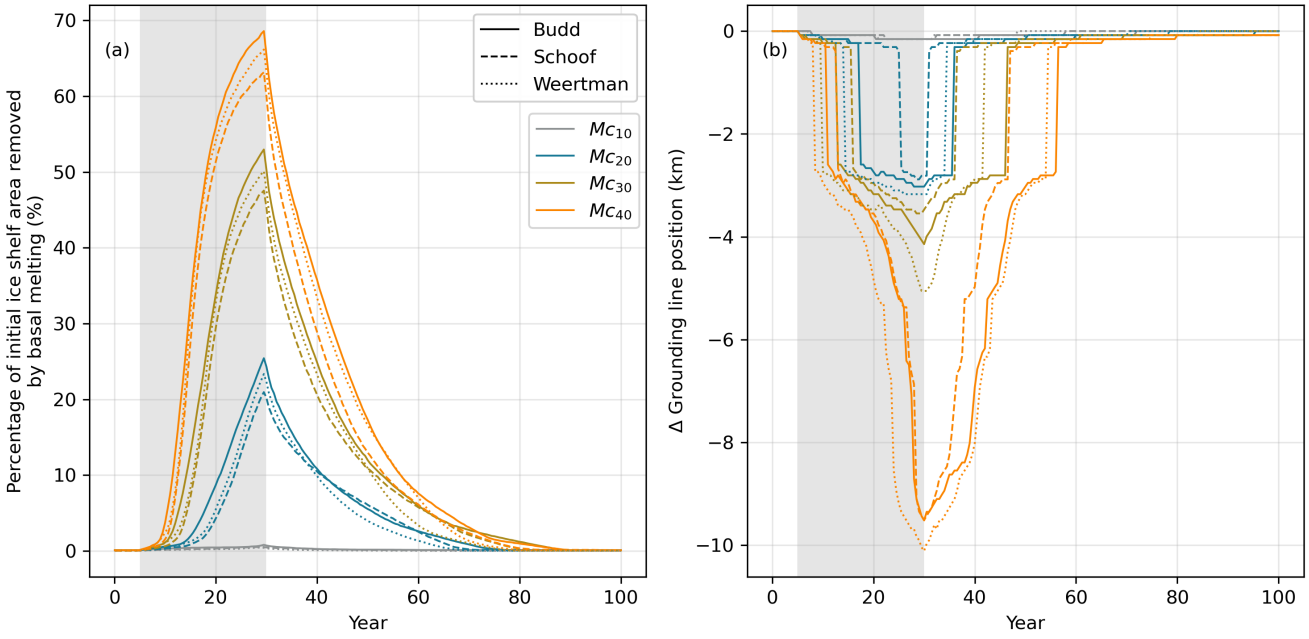

S 8: Constant melt rate (Mc) experiments. (a) Percentage of initial ice shelf area removed by basal melting. (b) Grounding line retreat along the central flowline shown in Fig. 2c. Negative numbers represent grounding line retreat and positive numbers represent grounding line advance, relative to the $Ctrl$ experiment. Grey shaded area denotes the perturbation period.